~~An integrated~~ A combined hydrological and hydraulic modelling approach for the flood ~~risk assessment over~~ hazard mapping of the Po river basin.

Rita Nogherotto[1], Adriano Fantini[1], Francesca Raffaele[1], Fabio Di Sante[1], Francesco Dottori[2], Erika Coppola[1], and Filippo Giorgi[1]

[1]International Centre for Theoretical Physics,Trieste, Italy
[2]European Commission, Joint Research Centre, Ispra, Italy

April 16, 2020

Abstract

Identification of flood prone areas is instrumental for a large number of applications, ranging from engineering to climate change studies, and provides essential information for planning effective emergency responses. In this work we describe ~~an integrated~~ a combined hydrological and hydraulic modeling approach for the assessment of flood-prone areas in Italy and we present the first results obtained over the Po river (Northern Italy) at a resolution of ~~90m~~90 m. River discharges are obtained through the hydrological model CHyM driven by GRIPHO, a newly-developed high resolution hourly precipitation dataset. Runoff data is then used to obtain Synthetic Design Hydrographs (~~SDHs~~S_{DH}) for different return periods along the river network. Flood hydrographs are subsequently processed by a ~~parallelized~~ parallel version of the CA2D hydraulic model to calculate the flow over an *ad hoc* re-shaped HydroSHEDS digital elevation model which includes information about the channel geometry. Modeled hydrographs and ~~SDHs~~ S_{DH} are compared with those obtained from observed data for a choice of gauging stations, showing an overall good performance of the CHyM model. The flood hazard maps for return periods of 50, 100, 500 years are validated by comparison with the official flood hazard maps produced by the River Po Authority (Adbpo) and with the Joint Research Centre's (JRC) pan-European maps. The results show a good agreement with the available official national flood maps for high return periods. For lower return periods the results ~~and~~ are less satisfactory but overall the application suggests a strong potential of the proposed approach for future applications.

Keywords: Flood hazard; Flood mapping; CHyM ~~hydrologic~~ hydrological model; CA2D hydraulic model.

1 Introduction

The last few decades have seen increased interest towards the study of floods, their consequences ~~and~~ on society and natural ecosystems and the development of measures to reduce their impact. Flood hazard maps are amongst the most important tools for flood risk management. According to the definition given by the European Floods Directive (European Commission, 2007), flood hazard maps are designed to indicate the probability and/or magnitude of ~~inundations~~ different flood scenarios over a given area and are used as ~~an important~~ a decision making tool for multiple purposes, ranging from infrastructure development to disaster response planning. ~~This is also endorsed by the European Union Flood Risk Management Directive(European Commission, 2007), which mandate is the development of~~ Following the requirements of the Floods Directive, all the member states of the European Union have developed river flood hazard maps~~for exposed territories, showing the potential consequences associated with different flood scenarios, in order to guarantee an effective basis for technical, financial and political decisions regarding the~~ , using the approach deemed to be most appropriate. Italy is frequently affected by severe inundation events caused by inland water bodies (Istituto di Ricerca per la Protezione Idrologica and Consiglio Nazionale delle Ricerche, 2018 , and this has led to the development of flood hazard maps already in the early 2000s under the responsibility of the local river basin authorities. The resulting national catalogue comprises flood maps developed with a considerable diversity of modelling approaches, data sets and coverage (ISPRA, 2017). In addition, the information on data and methods used is often difficult to retrieve and compare. As such, having a dataset at national scale developed with a uniform, consistent approach would allow a better comparison of flood ~~risk management. Until recently, flood hazard maps were only available for few regions of the globe, and with coarse resolutions, due to the high data and computational requirements of the hydraulic models employed in their production (Moel et al., 2009). The increase of computational power and the availability of remotely sensed datasets, however, have made the application of flood models with higher resolution (less than 1 km) possible even over large domains (Wood et al., 2011).~~ hazard across different areas, and improve national-scale analyses.

~~Different methods to quantify flood hazard can be employed, resulting in different types of flood maps (Moel et al., 2009). Within the different approaches, the common steps are essentially two: enumerate*1) the estimation of the discharges for specific return periods and the combination of the discharges with a digital elevation model (DEM) for the creation of the flood map. enumerate*For limited area gauged basins, where discharges data are available, the first step can be accomplished by using frequency analyses on discharge records and fitting extreme values distributions (e.g. Te Linde et al., 2008). For larger domains, flood information can be extrapolated to ungauged areas using regionalisation techniques (e.g. Merz and Blöschl, 2005) or by using hydrological models to calculate discharges (Bárdossy, 2007; Kha . These models require spatially explicit meteorological (e.g. temperature, precipitation, evaporation, radiation), soil, and land cover data as input and they solve the water balance for each geographical unit for each time step, to yield the discharges for all river stretches. The strength of this approach is not only the applicability over ungauged regions, but also~~

~~the possibility of assessing the impact of changes in climate and /or land cover on floods. The second step is usually accomplished by using hydraulic models specifically designed for solving channel and floodplain hydraulic routing. Historically, this was usually performed by modeling fluvial hydraulics with~~ Considerable portions of flood hazard maps in Italy were produced with one-dimensional ~~finite difference solutions of the full St. Venant equations (see Fread, 1985; Samuels, 1990), using models such as MIKE11 (Havnø et al., 1995) and HEC-RAS (Brunner, 2002). These schemes describe the river channel and floodplain as a series of cross sections perpendicular to the flow and estimate average velocity and water depth at each cross section. Despite the successful validation of flood inundation extent using low resolution satellite imagery (Bates et al., 1997), the one-dimensional schemes have the drawbacks of being computationally expensive and the areas between the cross sections are not explicitly represented (Samuels, 1990; Bates and De Roo, 2000).Thanks to the increasing availability of high resolution Digital Elevation Models (DEM) for floodplain areas,~~ hydraulic models (Autorità di bacino del fiume Po , 2012), mainly because of the limitations in topographic data and computational power. Today, two-dimensional ~~distributed models have been developed to allow a better conjunction with the elevation of the channel and of the floodplain surface, and to guarantee the calculation of the water depth and depth-averaged velocity at each computational node at each time step. Examples of such two-dimensional schemes are LISFLOOD-FP (Bates and De Roo, 2000), RBFVM-2D (Zhao et al., 1994) and TELEMAC-2D (Galland et al., 1991). These physically based models solve the Shallow Water Equations (SWEs) and, due to the recent advancement~~ (2D) models based on reduced complexity equations (i.e. where full flow equations are conveniently simplified; Bates et al. (2010)) can provide an adequate representation of flooding processes, generally outperforming one-dimensional models under a wide range of conditions (Horritt and Bates, 2002; Di Baldassarre et al., 20 . Moreover, due to huge advancements in parallel computing techniques, these models can be applied over large areas at high resolution~~. In recent years, a new approach was developed which employs cellular automata (CA) algorithms instead of directly solving the SWEs for each interface: for each timestep, the new state of a cell depends only on the state of the neighbouring cells at the previous timestep, according to a set of rules. This technique allows to model complex physical systems using simple operational rules (Wolfram, 1984), drastically reducing the computational requirements compared to physically based models. These algorithms are therefore well suited for parallel computation and have been successfully used to simulate many types of water related problems (e.g. Coulthard et al., 2007; Krupka et al., 2007; Au . An example is the CA2D model developed by Dottori and Todini (2011). The CA2D model uses a 2D cellular automata approach and the equations developed for the LISFLOOD-FP model (Bates et al. (2010)) to make high resolution simulations possible at continental and global scale (Dottori et al. (2016d)).~~ , thus making simulations possible at continental and even global scale (Sampson et al., 2015; Dottori et al., 2016d; Wing et al., 2017). Nevertheless, models based on global datasets still have important drawbacks, such as the inability to accurately represent river bed geometry due to the lack of global datasets of channel bathymetry (Yamazaki et al., 2019). Such limitations can be overtaken when focusing on data-rich areas, however, recent scientific studies on flood hazard estimation in Italy have mostly focused on examining specific limited areas of interest (Di Salvo et al., 2017; Marchesini et al., 2016; Morelli et al., 201 , particular past events (Amadio et al., 2013; Marchi et al., 2010; Masoero et al., 2013; Norbiato et al., 200 or flood risk rather than hazard (Albano et al., 2017; Salvati et al., 2010). In this study we describe ~~an integrated~~ a combined hydrological and hydraulic modelling approach which uses the Cetemps Hydrological Model (CHyM, Coppola et al. (2007)) and a modified version of the CA2D hydraulic model ~~, hereinafter~~ (Dottori and Todini, 2011), hereafter referred to as $\mathrm{CA2D}_{par}$. $\mathrm{CA2D}_{par}$ includes a parallel algorithm with the physics of the CA2D model ~~but that can be run with multiple processorsto further speed up the computation~~which allows the model to be run on multiple processors. Furthermore, to better represent river flow and flooding processes, we produced a re-shaped digital elevation model which includes information about the channel geometry ~~by simulating a "digging" assuming~~ based on a "digging" assumption stating that discharges associated to return periods of 1.5 years produce no floods, as they represent the conveyance capacity of the river channel. ~~This model has been used~~ The method we describe aims at finding a universal way to account for river channel geometry, also in regions where there is no available information about river natural banks. The use of a combined hydrological and hydraulic approach to calculate discharge (Bárdossy, 2007; Khan et al., 2011) has considerable advantages, such as the applicability over ungauged regions and the possibility of assessing the impact of changes in climate and/or land cover on floods. The proposed methodology has been applied over the entire Italian territory~~. In the present work~~ , however, for illustrative purposes, here we focus on the results obtained over the Po river ~~, which is the river with the~~ basin. The Po River exhibits the largest average daily discharge in the Italian peninsula~~and in whose basin~~ , and 40% of the gross domestic product of Italy is produced ~~(Montanari, 2012).~~ in its river basin (Montanari, 2012) . The Po River Basin Authority (AdbPo, www.adbpo.gov.it) provides flood hazard maps for the entire Po basin for three return periods (20-50, 100-200 and 500 years). These are relatively well documented and available for use (Autorità di bacino del fiume Po , 2012), thus providing a valuable benchmark for the procedure. In Section 2 we ~~will~~ describe the observational and ~~modelled data and~~ simulation data along with the method applied for flood hazard assessment of the western basin of the river Po. Section 3 ~~will present~~ presents the results, ~~by means of a validation of the obtained SDHs, a~~ including the validation of the Synthetic Design Hydrographs and the simulated ICTP2H flood hazard maps against observations and ~~against~~ existing flood hazard maps.

2 Data and methods

The approach proposed ~~herein assumes that large scale~~ here assumes that flood hazard maps over a large domain can be derived from an ensemble of small ~~scale simulations~~ sub-simulations of flood processes, arranged to cover the entire river network ~~, as previously demonstrated in literature~~ (Alfieri et al., 2013, 2014; Dottori et al., 2016d). The procedure is composed ~~by~~ of the following steps: 1) ~~the~~ hydrological simulations are setup and calibrated for the production of a long-term discharge time series; 2) ~~the~~ designed hydrographs are derived for different selected return periods; 3) ~~the~~ floodplain hydraulic simulations are performed and the flood maps for each return period are produced. These three ~~different steps will be~~ steps are described in detail in the following subsections.

2.1 The ~~observational~~ observation data and the hydrological model CHyM

Hydrological simulations are performed using the CETEMPS Hydrological Model (CHyM) (Coppola et al., 2007), ~~the~~ a distributed hydrological model developed by the ~~CETEMPS~~ Center of Excellence at the University of L'Aquila. CHyM uses information from a Digital Elevation Model (DEM) and ~~produces a~~ employs an eight flow direction (D8~~connected river network~~) approach (Tribe, 1992; Jenson and Domingue, 1988; Martz and Garbrecht, 1992), using cellular automata algorithms to resolve local singularities and no-flow points (Coppola et al., 2007). Input precipitation from various sources can be assimilated, including gridded precipitation from observations and models. Discharge is routed through each grid cell using continuity and momentum equations based on the kinematic shallow water approximation of Lighthill and Whitham (1955). Potential evapotranspiration is computed as a function of the reference evapotranspiration, which is the evapotranspiration in saturated soil conditions. For details about the computation of the reference evapotranspiration we refer to Todini (1996) and Thornthwaite et al. (1957). CHyM is specifically designed for Italian river catchments and has been widely tested for a variety of regions across Italy, and in particular for the Po basin (Coppola et al., 2014; Verdecchia et al., 2009; Tomassetti et al., 2005b)~~. For this study , nine separate domains are simulated, with a resolution varying between 300 and 900m (Fig. ??). The nine domains on which the CHyM model is run operationally. The domains are matching the~~ , the largest of the peninsula. The domain chosen for this study consists of the upper part of this catchment, and matches one of the nine operational domains simulated by CETEMPS to forecast potential floods over the Italian territory using stress indexes (Tomassetti et al., 2005a; Verdecchia et al., 2008)~~, but they are higher resolution because the HydroSHEDS Digital Elevation Model is used (Lehner et al., 2013), which is specifically conditioned for hydrological usage.~~ . The simulations performed for this study are part of a thesis project (Fantini, 2019, chapters 4) focused on the impact of climate change over flood hazard for the Italian territory. For details regarding the tuning and calibration of the model, we refer to the aforementioned thesis and to previous studies performed over this area (Coppola et al., 2014; Verdecchia et al., 2009; Tomassetti et al., 2005b), whose tuning parameters were used as a basis for the calibration of our simulations. In particular, a spatial resolution of 900 m, a spin-up time of 6 months and a timestep of 1.2 minutes for the solution of the prognostic continuity equation are employed. Testing with higher spatial and temporal resolutions did not result in an improved representation of river discharges when compared with observed data (Fantini, 2019). The choice of the DEM is crucial to ensure a correct river routing, especially in large, flat areas such as the Po plain. Our simulations are based on the HydroSHEDS Digital Elevation Model (Lehner et al., 2013), which is specifically conditioned for use in hydrology applications and offers very high resolution (around 90 m). The simulations span the period 2001–2016 and are driven by the newly-developed hourly precipitation dataset GRIPHO (Fantini et al., 2020; Fantini, 2019), which includes quality-controlled data from 3712 precipitation stations covering ~~all of Italy~~the Italian territory interpolated on a 12 km resolution grid. MM5 weather forecasts (Grell et al., 1994), operationally in use at CETEMPS for more than 20 years (see e.g. Bianco et al., 2006), are employed to fill data gaps in GRIPHO.

Further information on the hydrological simulations used for this study, including validation against discharge observations, can be found in Fantini (2019, chapters 4 and 5).

2.2 Processing the hydrological inputs: the Synthetic Designed Hydrographs ~~(SDHs)~~

The statistical procedure applied in this study is based on the work of Maione et al. (2003), who performed a Flood Frequency Analysis ~~(FFA)~~ starting from observational data for the Po river basin. The aim is to obtain curves describing the typical discharge ~~timeseries~~ time series of the event at ~~that~~ a river point for the given Return Period. These ~~$Q_{RP}(t)$~~ $Q_{R_P}(t)$ curves will be called Synthetic Design Hydrographs (~~SDHs~~S_{DH}) and they represent the discharge (Q) of a typical extreme event as a function of the Return Period (~~RP) and the~~ R_P) and time (t). ~~SDHs~~ S_{DH} are estimated and used as input data for the hydraulic model in order to ~~predict~~ calculate the corresponding maximum flood inundation extent and depth (see subsection 2.3). Simulations ~~were performed using observational~~ are performed using observed data described in subsection 2.1 and processed to derive synthetic flood hydrographs throughout a statistical analysis of the Flow Duration Frequency (FDF) reduction curves ~~$Q_D(RP)$~~$Q_D(R_P)$ (Maione et al., 2003) . These curves represent the typical discharge with Return Period ~~RP~~ R_P averaged over any duration D ~~around the flood peak~~ranging from 0 (the instantaneous discharge) to a value D large enough for the basin. For each station along the river network ~~$Q_D(RP)$~~ $Q_D(R_P)$ can be calculated from statistical analyses of historical hydrographs. ~~Similarly to the work of Maione et al. (2003) we used the empirical relationship proposed by NERC (1975) defining the reduction ratio (ϵ_D), which is the ratio of the FDF and the peak flood discharge ($Q_0(RP)$), as follows:~~

$$\epsilon_D(RP) = \frac{Q_D(RP)}{Q_0(RP)}.$$

~~In this work we assume ϵ_D is independent on the return period, which occurs for medium-large catchments, as done by Maione et al. (2003) and Alfieri et al. (2013).~~ When performing the calculation of the FDF around each historical flood peak, the centre of the duration window of width D is chosen as to maximise the average computed discharge Q_D:

$$FDF = Q_D = \frac{1}{D} \max \int_t^{t+D} Q(\tau) d\tau, \tag{1}$$

where t and τ represent time. The shape of the final synthetic hydrograph ~~will be~~ is determined by the peak-duration ratio r_D~~that is~~ , i.e. the ratio of the time before the peak and the total duration D of the averaging window. ~~The smaller the~~ An example of data sampling of Q_D and r_D ~~, the more skewed the hydrograph will be towards steeper (flatter)~~

~~rising (falling) limbs of the hydrograph~~from historical hydrographs is presented in Figure 1 of Maione et al. (2003). Centring on $t = 0$ the peak flood timing, the two limbs of the hydrograph can be described as:

$$\int_{-r_D D}^{t=0} Q(\tau) = r_D D Q_D(\underline{RP}R_P) \tag{2}$$

and

$$\int_{t=0}^{(1-r_D)D} Q(\tau) = (1-r_D) D Q_D(\underline{RP}R_P), \tag{3}$$

where ~~$Q_D(RP)$~~ $Q_D(R_P)$ is the typical FDF curve for the Return Period ~~RP. The construction of the SDH is performed imposing that the maximum discharges for each duration coincides with the value obtained from the FDF curves, in a given duration D for each value of the return period RP. Thus the SDH~~ R_P and the right-hand sides of Eqs. (2) and (3) represent the areas of two rectangles, before and after the peak, respectively (see Figure 1 in (Maione et al., 2003)). The smaller the r_D, the more skewed the hydrograph towards steeper rising limbs of the hydrograph and vice-versa for the falling limbs. The S_{DH} is obtained differentiating with respect to the duration D, following Maione et al. (2003), obtaining for the falling limb:

$$\underline{SDH}S_{DH} = Q_t(\underline{RP}R_P) = \underline{\frac{d/dD[(1-r_D)DQ_D(RP)]|_{D=D(t)}}{d/dD[(1-r_D)D]|_{D=D(t)}}} \frac{d/dD[(1-r_D)DQ_D(R_P)]|_{D=D(t)}}{d/dD[(1-r_D)D]|_{D=D(t)}} \tag{4}$$

where $t = (1-r_D)D$, $0 \leq t \leq (1-r_D)D$, and for the rising limb:

$$S_{DH} = Q_t(R_P) = \frac{d/dD[r_D D Q_D(R_P)]|_{D=D(t)}}{d/dD[(r_D D]|_{D=D(t)}} \tag{5}$$

where $t = -r_D D$, $-r_D D \leq t \leq 0$.
Similarly to the work of Maione et al. (2003) we used the empirical relationship proposed by NERC (1975) to define the reduction ratio (ϵ_D), i.e. the ratio of the FDF and the peak flood discharge ($Q_0(R_P)$), as follows:

$$\epsilon_D(R_P) = \frac{Q_D(R_P)}{Q_0(R_P)}. \tag{6}$$

Here we assume that ϵ_D is independent of the return period, a valid assumption for medium-large catchments, as done by Maione et al. (2003) and Alfieri et al. (2014). Based on this assumption, $Q_D(R_P)$ can be expressed through $Q_0(R_P)$. The maximum flood discharge ~~$Q_0(RP)$~~ $Q_0(R_P)$ for any given Return Period ~~RP must then be~~ R_P is then calculated by fitting an appropriate extreme distribution. Following Alfieri et al. (2015) and Maione et al. (2003), we chose the Gumbel distribution, so that:

$$Q_0(RP\,R_P) = u - \alpha \ln\left[-\ln\left(1-\frac{1}{RP}\frac{1}{R_P}\right)\right], \qquad (7)$$

where the parameters u and α are estimated from the fit, performed by means of the maximum likelihood estimation (MLE), and are used for the differentiation of the equation 5. The ~~equation~~equations, representing the falling ~~limb of the SDH, allows~~ and the rising limbs of the S_{DH}, allow us to calculate a typical flood event discharge ~~timeseries~~ time series for any location and Return Period, starting only from the ~~timeseries~~ time series of yearly maximum discharges. Further details about the procedure and its implementation can be found in ~~Fantini (2019).~~ Maione et al. (2003) and in Fantini (2019). As an example application of this procedure, Figure 1 shows ~~SDHs for seven Return Periods~~ S_{DH} for seven return periods obtained applying the procedure described in section 2.2 ~~for a~~ using data from the Farigliano station on the Tanaro river ~~, a tributary of the Po river.~~ in the South-Western part of the study area, whose data are taken from the European Water Archive (EWA, 2014) .

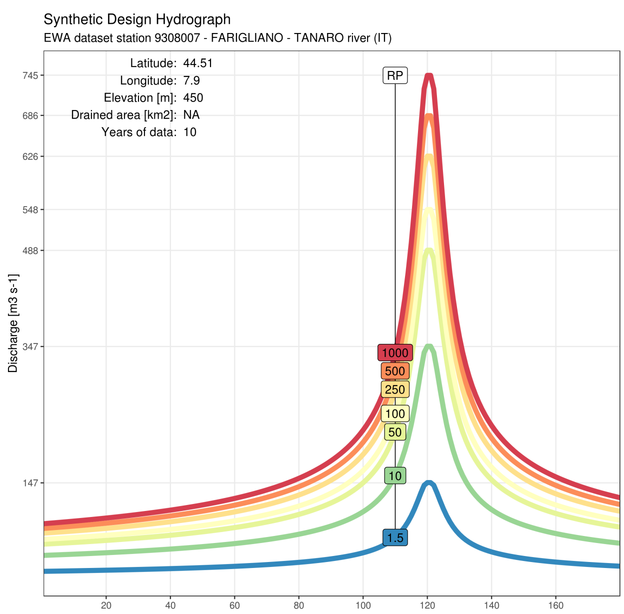

Figure 1: Example Synthetic Design Hydrograph computed following the procedure described in section 2.2 for a station on the Tanaro River, tributary of the Po river. Seven Return Periods (1.5, 10, 50, 100, 250, 500 and 1000 years) are shown.

2.3 Modelling the flood inundation: the hydraulic model

Floodplain hydraulic simulations are performed with a modified version of the 2D hydraulic ~~cellular automata~~ model CA2D ~~. The model , described and validated in Dottori and Todini (2011)~~

~~, is based on a simple cell-centred finite volume scheme, which uses the Euler explicit scheme for the integration in time. The momentum equation is solved for each time step, computing volume exchanges between grid cells along the cell's borders. Volumes of each cell are successively updated using volume conservative equations. For this study, the model is run using the~~ Dottori and Todini (2011). We use as starting point the model version proposed by Dottori et al. (2016d), which adopts a raster computation grid with an 8-direction link network (Moore neighbourhood rule, Parsons and Fonstad (2007)) and the semi-inertial formulation of the ~~momentum equation (Bates et al. (2010)), which allows to reproduce channel and floodplain flow processes with a good level of detail with a considerably reduced computational effort (Dottori and Todini, 2011). The model version CA2D$_{par}$ has been written using Fortran90 standard and it has the original modeldescribed in Dottori and Todini (2011) as a starting point. The physics is represented on a cartesian 2D grid that allows a good level of scalability. The parallel code has been carried out using the message passing interface (MPI) communications. A number of subroutines has been introduced in the code to deal with the parallelization and are compiled as separated modules.~~ momentum equation (Bates et al. (2010)). Note that the model uses the same flow equations for both the channel flow and floodplain flow. The model code was parallelized using the message passing interface (MPI) communications. In this new version, hereinafter referred to as $CA2D_{par}$, the physics is unchanged with respect to the original version but the code was translated into a more recent fortran standard (Fortran90), with a number of new subroutines. To evaluate the performance and scalability of the model, a set of 11 different simulations were carried out and the wall clock times in seconds as a function of number of cores are reported in Figure 2. The domain used for the scalability tests has a spatial extension of 0.3 by 0.3 degrees with a resolution of 90 meters. The tests were run on the ICTP HPC cluster (Argo http://argo.ictp.it/) with 36 nodes each having 12 Sandybridge Cores and 32 GB per node. The number of cores used for the tests span from 12 to 120 with a step of 12. The parallelization of the code increases as expected the performance of the model ~~which is~~ by a factor of up to 7.5 times ~~faster~~ with respect to the original model, even with a limited number of cores~~(Fig.~~. The speed increases with the number of cores up to 60 cores, when the best performance is reached (Figure 2).

~~The flood inundation extent is dependent on the spatial extent of the performed hydraulic simulations, and it is therefore important to define the number and location of the hydraulic simulation in order to achieve the full coverage of the interested river network. The following section will show the results obtained and it is organised in three steps: enumerate*1) calculation of the design flood hydrographs for the available observational stations along the river network using observational data, calculation of the design flood hydrographs obtained using the CHyM model data on the same locations, and comparison of the two series of hydrographs for a validation of the hydraulic model along the Po river, calculation of the design flood hydrographs in selected points along the river network at regular distance from each other and performance of the CA2D$_{par}$ simulations using the SDH as inputs. enumerate*~~

2.4 ~~The production of the flood maps.~~

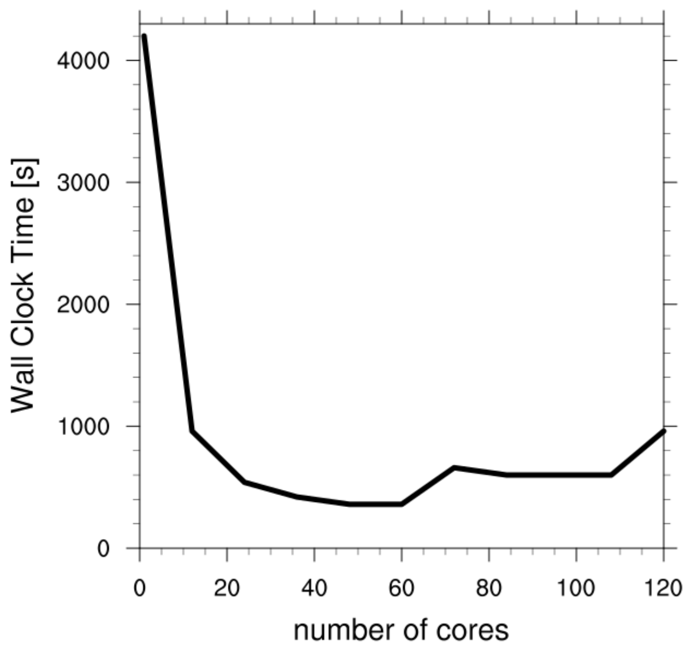

Figure 2: Wall-clock time (s) variation with the number of cores achieved with the parallelization of the CA2D model.

~~Currently the~~

2.4 The production of the ICTP2H flood maps.

2.4.1 The Digital Elevation Model

Currently, the Shuttle Radar Topography Mission (SRTM) digital elevation model (Farr et al., 2007; Rabus et al., 2003) is considered as one of the best openly available ~~data set~~ datasets for flood modeling ~~offering~~ with near-global ~~converage~~ coverage (Hirt et al., 2010; Jing et al., 2014). The void-filled HydroSHEDS variant of SRTM was used in this work with 3 arc sec resolution (Lehner et al., 2006, 2008).

2.4.2 The "digging method"

As described in Neal et al. (2012) and Sampson et al. (2015) the inclusion of a river channel network is necessary to guarantee acceptable results in the simulation of flood depths and extent. River widths and depths are however difficult parameters to estimate ~~as it is not possible to measure them remotely on large scales.~~ remotely for larger domains (Yamazaki et al., 2014). In particular, direct or indirect measures of channel depth and section are not yet available. Natural and artificial river defenses are also challenging to incorporate as their features are smaller than the model grid resolution (Sampson et al., 2015). Moreover their spatial distribution on large scales is not available~~as literature about~~, as the literature on fluvial flood defenses generally refers to individual sites (e.g. Brandimarte and Di Baldassarre, 2012; Te Linde et al., 2011). Available remotely sensed data were recently used to generate regional to global estimates of river widths and depths (Andreadis et al., 2013; Gleason and Smith, 2014) by coupling river network data to web based imagery services such as Google maps or Bing maps.

In ~~this study we have used~~ order to estimate the channel conveyance, here we use the near-global database of bankfull depths, based on hydraulic geometry equations and the HydroSHEDS hydrography ~~data set~~ dataset described in Andreadis et al. (2013)~~, to estimate the channel conveyance. The~~. The novel idea is to link the channel geometry to the discharge return period, as it guarantees that channels, properly sized, are able to contain the simulated flows~~and moreover mitigates against~~. The method also mitigates the problem of missing information ~~about the~~ on river banks. ~~We have used the river bankfull depths information to reshape the HydroSHEDS digital elevation model by assuming a bankfull discharge return period of 1.5 years (~~Leopold~~,~~ 1994~~;~~ Harman et al.~~,~~ 2008~~;~~ Andreadis et al.~~,~~ 2013~~;~~ Sampson et al.~~,~~ 2015~~;~~ Neal ~~.~~In order to include information about the geometry of the river ~~, the natural and man-made banks, we used~~ we use the bankfull depths to artificially "dig" the HydroSHEDS DEM~~until we obtained a no-flood map correspondent to the~~. We assign to each river segment of depth d_o given by Andreadis et al. (2013) a new depth d_n proportional to the original depth d_o according to:

$$d_n = k_d d_o \tag{8}$$

where k_d is the digging coefficient parameter chosen to minimize the flood extent corresponding to the return period of 1.5 years, which represents the conveyance capacity of the river channel ~~.~~ (Leopold, 1994; Harman et al., 2008; Andreadis et al., 2013; Sampson et al., 2015; Neal et al., 2012)

. This new depth is then subtracted to the HydroSHEDS digital elevation model. Digging the channel is applied to include the river bed permanently covered by water, which is not represented in the DEM. Conversely, representing embankments would require to “raise” DEM pixels corresponding to river banks in order to reproduce the blockage effect (as done by Wing et al. (2017)). The same could be done over the Po River where the level of flood protection is known, but this is not the case in a majority of river basins in Italy and Europe. Given that our goal is to develop a methodology applicable everywhere, we opted for not using local information for the model setup.

2.4.3 The “virtual stations”

As stated in 2.1 a 15-years continuous discharge time series with ~~Italian coverage~~ coverage of the Italian territory is generated using the CHyM hydrological model from January 2001 to December 2016. Floodpeaks with 50, 100, 500 year return period are derived for each river point in the model and downscaled to the river network at 3 arc sec resolution. Design flood hydrographs are then used to perform small scale floodplain hydraulic ~~simulation~~ simulations on points which will be hereafter referred to as “virtual stations” (see ~~Fig. 3),~~ Figure 3). These are located every 10 km along the river network ~~,~~ for rivers with drainage areas larger than A=5 km^2, using the hydraulic model CA2D$_{par}$. For each virtual station the simulation ~~was~~ is run over a sub-domain, 0.3°× 0.3°, chosen to optimise the computational effort, as the simulation time is strongly affected by the size of the domain. For each return period, a total of 474 simulations were performed and merged to produce a Western Po river flood hazard map (~~Fig. 4).~~ Figure 4), taking the maximum depth value where more maps overlap. In each computation domain, roughness values for the hydraulic simulations are derived from the Corine Land Cover map (Copernicus Land Monitoring Service). The range of values goes from 0.2 m 1/3 s for forest areas to 0.04 m 1/3 s for river channels, following the values used in (Alfieri et al., 2015). In all the simulations a free flow boundary condition is assumed at the edge of each domain, while the initial water level for the sea and internal water bodies is given by the local DEM value. We do not include levees in the model domain, as the information on their geometry is not available from remotely sensed datasets, therefore we assume that overflow occurs when channel conveyance is exceeded.

3 Results

3.1 Validation of the ~~SDHs.~~Synthetic Design Hydrographs

~~Tuning and testing of the method were performed~~ The method was tested on the upper Po basin ~~,~~ due to previous experience with the hydrological model ~~on~~ in this domain (Coppola et al., 2014) ~~,~~ and the availability of reliable observed discharge data ~~, and lack of large water management structures~~(Fantini, 2019). Due to the relatively small size of the simulated ~~domains,~~ domain, 0.3°× 0.3°, the duration of all flood simulations was set to 240 h. The ~~SDHs were validated using data from the CHyM model and~~ S_{DH} were first produced using observations from 31 gauge stations along the Po river provided by CETEMPS, and therefore compared with those obtained using the CHyM model at the same stations. Figure 5 shows the results of the comparison between ~~the SDHs obtained with observational data and those~~

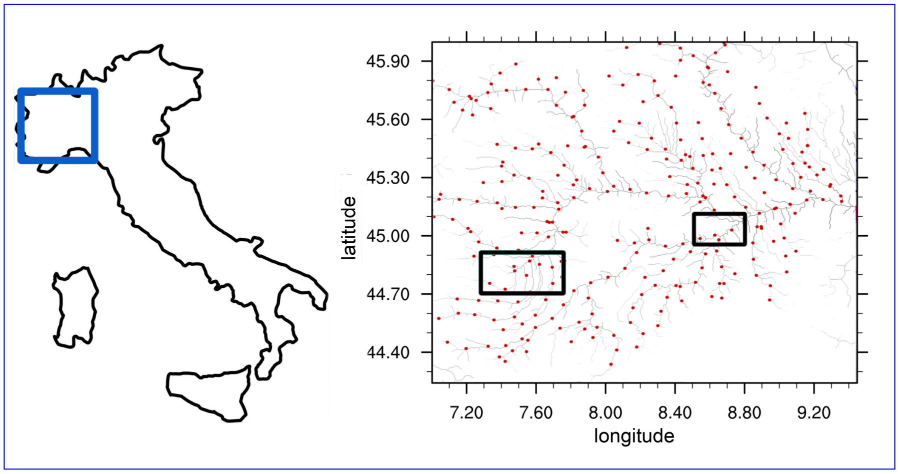

Figure 3: Virtual stations selected for drainage areas larger than A=5 km^2 and regularly spaced every 10 km along the high-resolution river network of the analyzed domain (blue box on the left). Black square boxes show the flooded area analyzed in subsection 3.2.

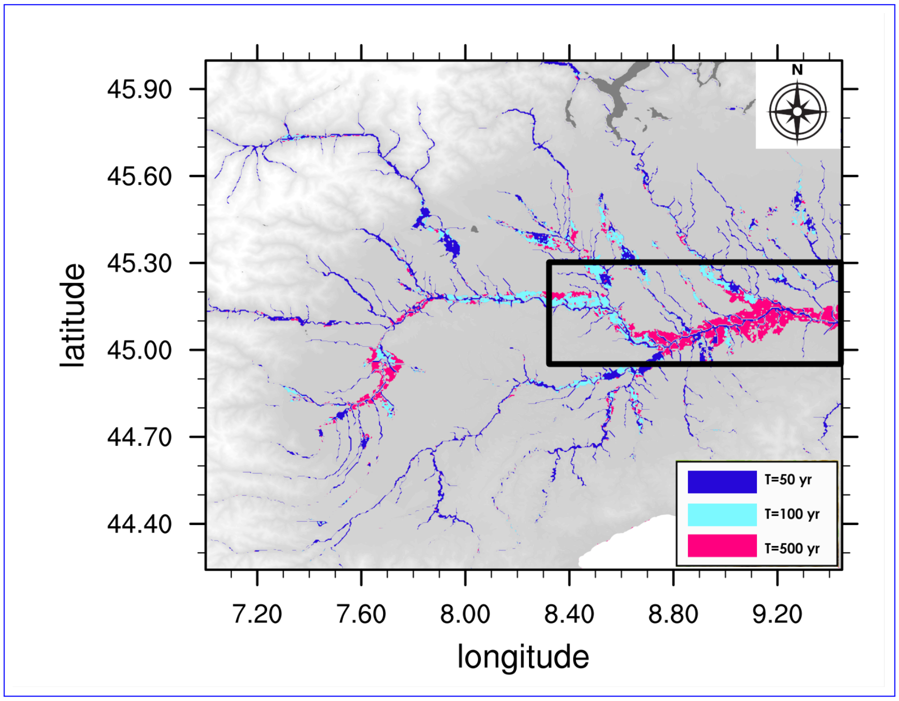

Figure 4: Western Po river flood hazard map for the Return Periods of 500, 100 and 50 years obtained using the CHyM hydrological model and the $CA2D_{par}$ hydraulic model combined. The black box indicates the area analyzed for comparison in subsection 3.3.

~~obtained with modelled data. The SDHs~~ observed and simulated S_{DH} values. The S_{DH} are generally closely ~~approximated~~ reproduced by the model, both in ~~the peaks and in the area of~~ terms of peaks and area under the curves. The coefficient of determination (R^2) between observed and simulated data is 0.85 for the ~~SDHs~~ S_{DH} areas and 0.92 for the ~~SDHs peakswhich are the same values~~ S_{DH} peaks, which are similar values to those reported in Rojas et al. (2011) for a hydrological model ~~of~~ for Europe without bias correction of climate data and in ~~Paprotny et al. (2017)~~?.

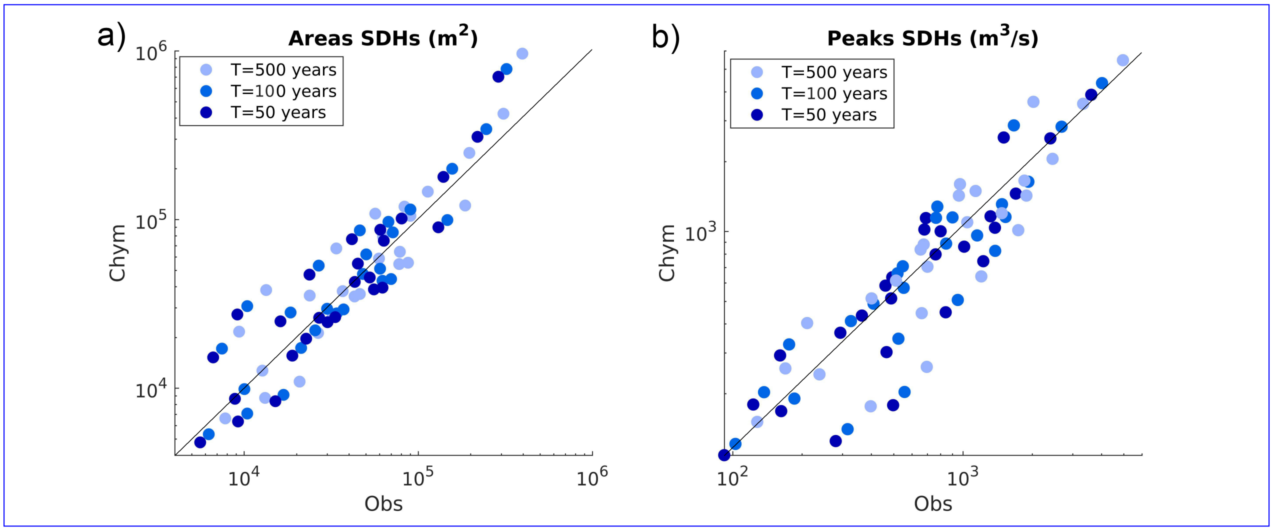

Figure 5: Comparison of simulated (CHyM) and observed (Obs) ~~SDHs~~ S_{DH} areas (a) and discharges peaks (b) for 31 gauge stations along the Po river, for three return periods.

3.2 Comparison against observations: a case study

Validation of flood hazard models is achieved ~~trough~~ through the evaluation of the model accuracy in estimating the probability of flood occurrence and ~~the evaluation~~ of relevant hazard variables ~~of~~ for an event (e.g. flood extent and depth, flow velocity). Unfortunately the evaluation is strongly limited by the scarce availability of reference flood maps and flood observations, and is a key topic in flood risk analysis. Various methods were suggested by previous studies. One consists in comparing the ~~produced~~ simulated maps with previous maps based on the statistical estimation of peak discharges (Pappenberger et al., 2012); another method performs a qualitative assessment of the flood events against satellite flood images (Rudari et al., 2015).

In order to ~~perform a first validation of the~~ provide a quick evaluation of our flood hazard mapping methodology we consider a case study of a flood recently occurred in Northern Italy~~, catalogued as an event with return period of 100 years~~. Even though such exercise is not a formal validation (as in Section 3.3), it is presented to provide an evaluation of our methodology against a real flood event. November 2016 was characterized by a heavy ~~rainfalls~~ rainfall event involving the territory of North West of Italy, in particular the Regions

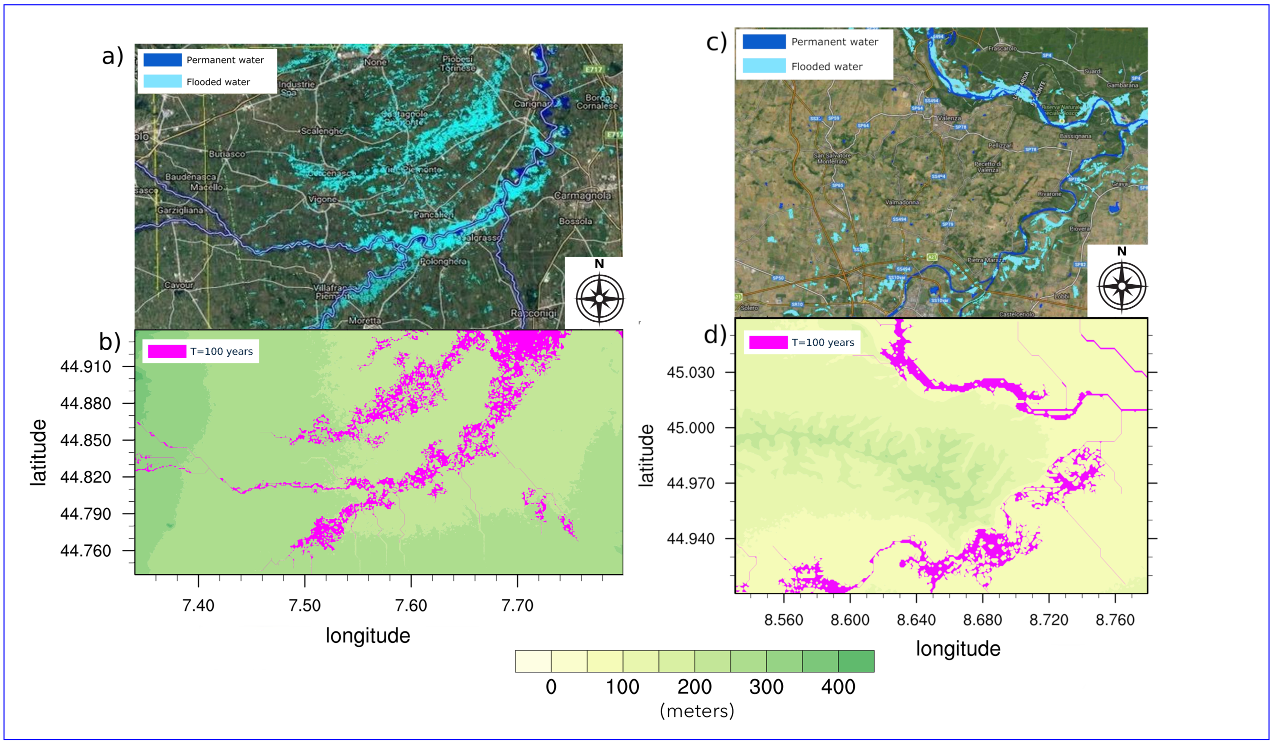

Figure 6: Case ~~studies~~ study in November 2016, used for the validation of the method: panels above show floods as acquired by the satellite COSMO-SkyMed (COSMO-SkyMed Image ©ASI (2016). All rights reserved). Panels below show floods as modelled by the ~~integrated~~ combined CHyM-CA2D$_{par}$ method. Panels (a) and (b) show flooded areas in the south of Turin. Panels (c) and (d) show flooded areas in the area of Alessandria.

of Piemonte and Liguria. The bad weather conditions and the persistence of ~~precipitations~~ intense precipitation caused the increase of hydrometric levels of all the rivers in these regions, and in particular in the Po river basin. According to local reports, the discharge recorded during the event may have reached a return period of 100 years.

Figures 6 (a) and (c) show the ~~images from~~ permanent and flooded water for a 36x20 km area South of Turin and a 20x15km area North of Alessandria, along the Po and the Tanaro rivers (the areas are indicated with the black squares in Figure 3). The images are provided by the satellite COSMO-SkyMed (CSK) (Covello et al., 2010), a four-satellite constellation which gives the possibility of acquiring X -band Synthetic Aperture Radar (SAR) data during day and night, regardless of weather conditions~~and is fully operational since the 2008.~~. It provides radar data characterized by short revisit time and therefore useful for flood mapping evaluation. Unfortunately, the data necessary for reproducing these images and assessing a first order performance of the methods using quantitative metrics are not currently available as the COSMO-SkyMed only provides these images in graphical format. The lower panels show the ICTP2H flood maps corresponding ~~to two different return periods (T=500 and T=~~the a return period of 100 years~~)~~. We can see that the observed event ~~, associated to a return period of 100 years, is fairly good~~ is fairly well represented by the model (~~Fig.~~ Figure 6 (b) and (d))~~as the maps include the particular events observed .~~, as the simulated maps include this particular observed event.

3.3 Comparison against existing flood hazard maps

Another approach for the validation ~~is to perform an evaluation against~~ of our method is to carry out a comparison with existing high-resolution flood hazard maps (Alfieri et al., 2013; Sampson et al., 2015; Winsemius et al., 2016). The evaluation of simulated ICTP2H flood maps against reference maps is performed using ~~the~~ indexes proposed in literature (Dottori et al., 2016d; Bates and De Roo, 2000; Alfieri et al., 2014). The Hit Ratio index (~~HR~~H_R), defined as:

$$\cancel{HR}H_R = (F_m \cap F_o)/(F_o) \tag{9}$$

evaluates the agreement of ~~modelled~~ CA2D flood maps (F_m) with existing maps (F_o). This index does not take into account the overprediction ~~and~~ or underprediction of the flooded area, therefore two other measures are calculated to account for this: the False Alarm index (~~FA~~F_A), defined as

$$\cancel{FA}F_A = [F_m - (F_m \cap F_o)]/(F_o) \tag{10}$$

where $F_m - (F_m \cap F_o)$ is the flooded area wrongly predicted by the model, and the Critical Success index (~~CS~~C_S), defined as:

$$\cancel{CS}C_S = (F_m \cap F_o)/(F_m \cup F_o). \tag{11}$$

The ~~produced~~ simulated ICTP2H flood hazard maps, ~~hereinafter~~ hereafter referred to as "~~CA2D~~ ICTP2H maps", are tested against the official hazard AdbPo flood maps~~(http://www.adbpo.gov.it)~~,

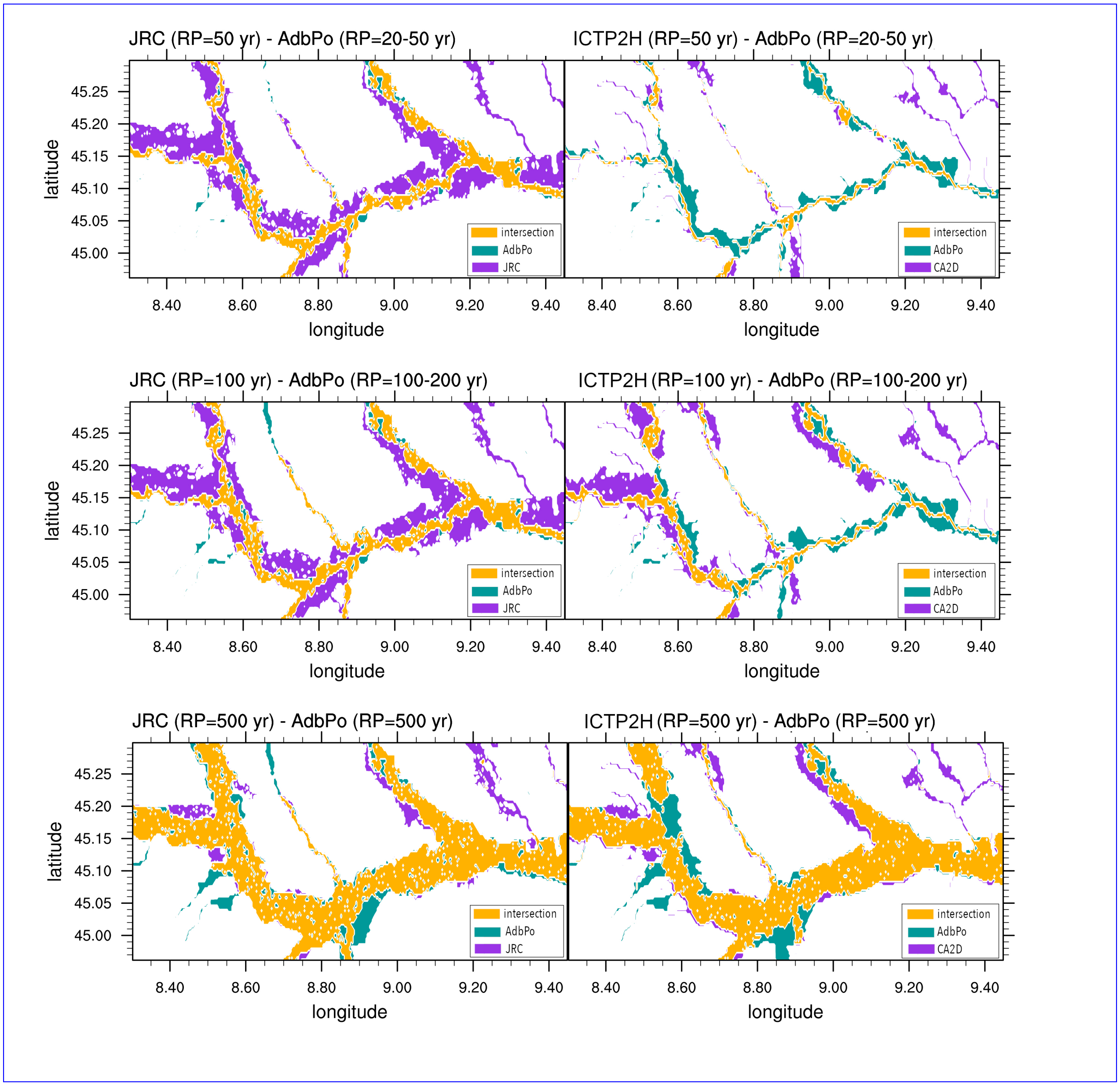

Figure 7: ~~Adbpo, JRC~~ ICTP2H and ~~CA2D~~ JRC flood hazard maps for the 50 years return period (upper panels), 100 years return period (central panels) and 500 years return period (lower panels) compared to AdbPo flood hazard maps for the 20-50, 100-200 and 500 years return period.

produced by the ~~River Po Authority, who classifies the flood~~ Po river basin Authority. According to the available technical documentation (Autorità di bacino del fiume Po , 2012) , the flood hazard maps related to the main river networks were calculated using 1D hydraulic models, integrated by 2D simulations in specific areas of interest (e.g. near bridges or hydraulic structures). All simulations were based on surveyed topography and river bathymetry. The delineation of flood-prone areas outside of river embankments were derived using GIS interpolation and considering terrain altimetry and geomorphologic features. The AdpPo maps classify the flood plain of the Po river into three levels corresponding to return periods of 20-50 years (high frequency), 100-200 years (medium frequency) and 500 years (low frequency).

In addition, we compare the ~~CA2D~~ ICTP2H maps with the flood hazard maps produced by the Joint Research Centre of the European Commission (JRC)~~. The JRC maps~~ , which are freely available online and are based on streamflow data from the European Flood Awareness System (EFAS (Demeritt et al., 2013) ~~and also calculated with~~ at a spatial resolution of 3" (Dottori et al., 2016a,b,c). A detailed description of the JRC modelling framework is reported by (Alfieri et al., 2014) and (Alfieri et al., 2015). While the JRC and our framework share a number of methods (e.g. to determine flood hydrographs and calculate flood maps), they use different models and datasets and diverge in other modelling solutions. For instance, the conveyance of the river channel is derived here using the "digging method" (described in Subsection 2.4.2), while the JRC flood maps account for this effect by removing 2-year return period discharge. To perform the ~~indexes~~ index calculations, we ~~have focused~~ focus our analysis on a smaller portion of the domain, centred on the main river, removing flooded areas originating from river sections with an upstream area smaller than 500 km^2, since they are not simulated and therefore not included in the JRC maps. ~~The JRC flood maps used for the comparison do not consider flood defences and river geometry, for~~ Neither the JRC nor ICTP2H maps consider the embankment system, since they are not represented in the DEMs used in the two studies. According to the available information (Autorità di bacino del fiume Po , 2012), the embankment system of the Po river is designed to allow flooding only in a limited portion of the river floodplain (i.e. the berms) for discharges with return periods up to 200 years. For this reason we only calculate the performance indices (Eq. (9), (10) and (11)) for the 500 years return period, reported in Table 1, since by construction any statistical evaluation for return periods calculation below RP 500y has no significance. Indices are calculated for the ~~CA2D~~ ICTP2H and JRC maps (F_m) against the Adbpo maps (F_o).

As can be seen, the ~~CA2D~~ ICTP2H maps provide fairly good results for the 500 years return period, with a ~~HR~~ H_R of 0.76, a ~~CS~~ C_S index of 0.67 and a very low false alarm value (0.12), while results are less satisfactory for lower return periods, with considerable underestimation of flood extent with respect to the ~~offical~~ official maps (see ~~Fig.~~ Figure 7). The JRC maps also show fair results for the 500 years return period, with a ~~HR~~ H_R of 0.83, a ~~CS~~ C_S of 0.73 and ~~FA~~ F_A of 0.15, and are similar to ~~CA2D maps (Fig.~~ the ICTP2H maps (Figure 8), but they systematically overestimate the flood extent for the lower return periods (see

	Hit Rate	False Alarm	Critical Success
JRC	0.83	0.15	0.73
ICTP2H	0.76	0.12	0.67

Table 1: Evaluation of the ~~CA2D~~ ICTP2H and JRC flooded extent against official flood hazard maps (Adbpo) for ~~thre~~ three return period of 500 years.

~~Fig.~~ Figure 7). The differences between ~~modelled~~ simulated and official maps are partly due to the topography of the Po floodplain, which is not reproduced in the ~~STRT~~ SRTM used by both ~~JRC and CA2D~~ the JRC and ICTP2H maps. Indeed, the area enclosed by the main levees has a complex system of minor embankments, which are designed for lower flood return periods than the main levees (Castellarin et al., 2011a). This explains why the AdBPo maps are quite similar for return periods of 20-50 years and 100-200 years (see Figure 7).

The narrow extent of flooded areas for return periods of 50 and 100 years in sectors of the river network suggests that the channel conveyance may be overestimated in ~~CA2D~~ the ICTP2H maps. However also our reference AdBPo maps show very similar flood extents for return periods of 20-50 and 100-200 years~~as explained above~~, therefore the ~~CA2D underestimation~~ underestimation ICTP2H can not be quantified. Future work will ~~anyway~~ be needed to refine the methodology of channel ~~"digging"~~ "digging". This is indeed an open research question, due to the absence of large-scale methods or datasets to estimate river channel depth (Dottori et al., 2016d). Nevertheless, it is worth noting that the method presented here improves the sensitivity ~~to return period of~~ of the flood extent maps to the return period. Conversely, the JRC maps calculated for different return ~~period~~ periods have limited differences, ~~due to the absence of river geometry details~~probably due to lack of flood defences in the model. These results confirm that the inclusion of a river channel network is necessary to guarantee acceptable results in the simulation of flood depths and extent for all return periods (Neal et al., 2012).

4 Conclusions

In this paper we investigate the feasibility of producing high-resolution flood maps using an innovative approach which reshapes the digital elevation models by ~~simulating a "digging"assuming that~~ a "digging" procedure that assumes that no floods take place for discharges associated to the return period of 1.5 years, thus representing the conveyance capacity of the river channel. ~~The~~ Although we are aware that for example most of the river networks in Europe have an average protection level of 100y RP (Rojas et al., 2013; Paprotny et al., 2017), the main purpose of this method ~~development is~~ is i) to be able to apply it also in those regions where there ~~are~~ is no available information about river natural ~~and man-made banks.~~

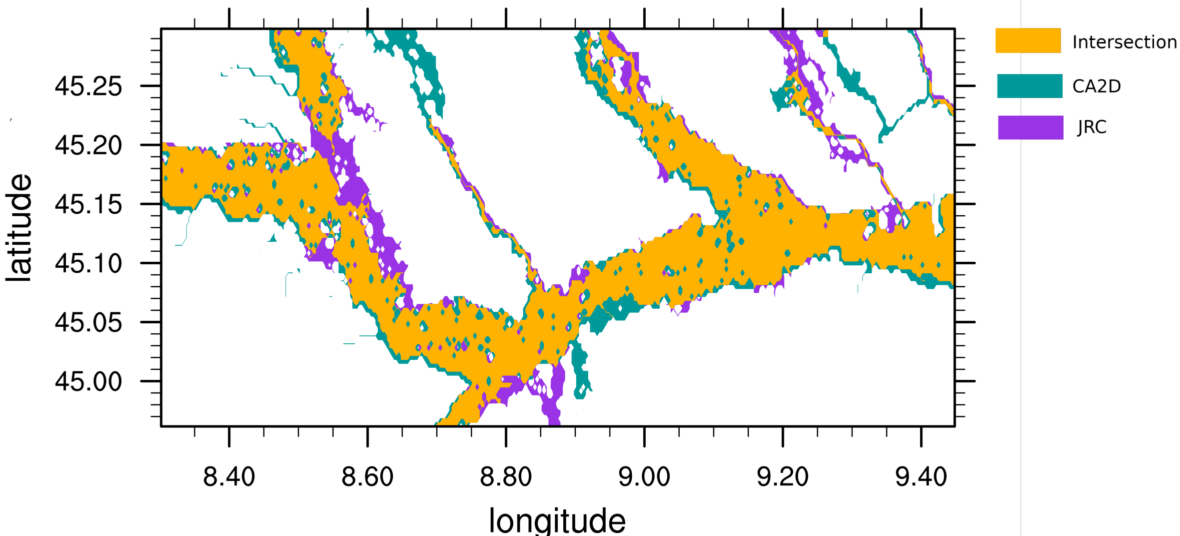

Figure 8: ~~CA2D~~ ICTP2H and JRC flood hazard maps for the 500 years return period

~~A~~ banks; and ii) to be able to use the method in a climate projection mode, estimating possible changes of any return period for each rivers segment. To this aim a 2-dimensional hydraulic model is used to simulate the propagation of ~~the hydrographs~~ water across the HydroSHEDS~~void filled DEM~~, which was processed to yield an estimate of bankfull discharge. The evaluation of ~~the produced flood maps was performed through some case studies of observed flood extent satellite data, and through existing~~ flood maps ~~over the entire domain, showing~~ produced with this method was carried out through existing official flood maps from the Po river basin authority (Adbpo) over a portion of the domain. We also compared our results with on additional dataset of flood maps produced at the JRC using a previous version of the hydraulic model. By construction, the assessment against Adbpo flood maps can only be carried out for the 500y RP and this showed a good spatial agreement ~~with observations for high return periods. Comparison for lower return periods showed that~~ between the ICTP2H and Adbpo flood area extent. Moreover, we showed how the DEM-reshaping method improves the sensitivity ~~to return period of~~ of the ICTP2H flood extent maps ~~but needs further improvement, for instance, combining observed data about~~ to the return period compared to the JRC maps, although this may be further improved by the combined use of observed data of the river bed depth~~and~~, width and discharge (Yamazaki et al., 2014). The ~~validation of the method in a region where all the~~ reason for the choice of the upper Po river basin in our study was due to high density of data available, however the method was developed for application to larger domains, such as the Italian or European regions. In fact, the method can be especially useful for regions around the world where most of the basins are ungauged and there is no information available on the protection levels. Future work entail the application of our method to larger regions using information from regional climate downscaled scenario simulations as input for the hydrological and hydraulic ~~information are available will allow us to extend the method elsewhere~~models. This will provide useful information for policy makers on how the present day flood return period may change in future scenarios, information that will be crucial for adaptation and mitigation strategy development such as, for example, the construction of new river bank protection.

5 Acknowledgments

The authors gratefully acknowledge the financial support of the Allianz Insurance Company for the realization of this project.

References

Albano, R., Mancusi, L., and Abbate, A.: Improving flood risk analysis for effectively supporting the implementation of flood risk management plans: The case study of “Serio” Valley, Environmental Science & Policy, 75, 158–172, 2017.

Alfieri, L., Burek, P., Dutra, E., Krzeminski, B., Muraro, D., Thielen, J., and Pappenberger, F.: GloFAS-global ensemble streamflow forecasting and flood early warning, Hydrology and Earth System Sciences, 17, 1161, 2013.

Alfieri, L., Salamon, P., Bianchi, A., Neal, J., Bates, P., and Feyen, L.: Advances in pan-European flood hazard mapping, Hydrological processes, 28, 4067–4077, 2014.

Alfieri, L., Burek, P., Feyen, L., and Forzieri, G.: Global warming increases the frequency of river floods in Europe, Hydrology and Earth System Sciences, 19, 2247–2260, 2015.

Amadio, M., Mysiak, J., Pecora, S., and Agnetti, A.: Looking Forward from the Past: Assessing the Potential Flood Hazard and Damage in Polesine Region by Revisiting the 1950 Flood Event, 2013.

Andreadis, K., Schumann, G., and Pavelsky, T.: A simple global river bankfull width and depth database, Water Resources Research, 49, 7164–7168, 2013.

Austin, R., Chen, A., Savic, D., and Djordjevic, S.: Fast Simulation of Sewer Flow using Cellular Automata, NOVATECH 2013, 2013.

Autorità di bacino del fiume Po : Progetto di Variante al PAI: mappe della pericolosità e del rischio di alluvione (in Italian), https://pianoalluvioni.adbpo.it/progetto-esecutivo-delle-attivita/, accessed on 2020-04-03, 2012.

Bárdossy, A.: Calibration of hydrological model parameters for ungauged catchments, Hydrology and Earth System Sciences Discussions, 11, 703–710, 2007.

Bates, P. and De Roo, A.: A simple raster-based model for flood inundation simulation, Journal of Hydrology, 236, 54–77, 2000.

Bates, P., Horritt, M., Smith, C., and Mason, D.: Integrating remote sensing observations of flood hydrology and hydraulic modelling, Hydrological Processes, 11, 1777–1795, 1997.

Bates, P., Horritt, M., and Fewtrell, T.: A simple inertial formulation of the shallow water equations for efficient two-dimensional flood inundation modelling., Journal of Hydrology, 387, 33–45, 2010.

Bianco, L., Tomassetti, B., Coppola, E., Fracassi, A., Verdecchia, M., and Visconti, G.: Thermally driven circulation in a region of complex topography: Comparison of wind-profiling radar measurements and MM5 numerical predictions, Annales Geophysicae, doi: 10.5194/angeo-24-1537-2006, 2006.

Brandimarte, L. and Di Baldassarre, G.: Uncertainty in design flood profiles derived by hydraulic modelling, Hydrology Research, 43, 753–761, 2012.

Brunner, G.: Hec-ras (river analysis system), in: North American Water and Environment Congress & Destructive Water, pp. 3782–3787, ASCE, 2002.

Castellarin, A., Di Baldassarre, G., and Brath, A.: Floodplain management strategies for flood attenuation in the river Po, River Research and Applications, 27, 1037–1047, 2011a.

Castellarin, A., Domeneghetti, A., and Brath, A.: Identifying robust large-scale flood risk mitigation strategies: A quasi-2D hydraulic model as a tool for the Po river, Physics and Chemistry of the Earth, Parts A/B/C, 36, 299–308, 2011b.

Copernicus Land Monitoring Service: Corine Land Cover., http://land.copernicus.eu/pan-european/corine-land-cover, accessed on 2020-04-08.

Coppola, E., Tomassetti, B., Mariotti, L., Verdecchia, M., and Visconti, G.: Cellular automata algorithms for drainage network extraction and rainfall data assimilation, Hydrological Sciences Journal, 52, 579–592, 2007.

Coppola, E., Verdecchia, M., Giorgi, F., Colaiuda, V., Tomassetti, B., and Lombardi, A.: Changing hydrological conditions in the Po basin under global warming, Science of the Total Environment, 493, 1183–1196, 2014.

Coulthard, T., Hicks, D., and Van De Wiel, M.: Cellular modelling of river catchments and reaches: advantages, limitations and prospects, Geomorphology, 90, 192–207, 2007.

Covello, F., Battazza, F., Coletta, A., Lopinto, E., Fiorentino, C., Pietranera, L., Valentini, G., and Zoffoli, S.: COSMO-SkyMed an existing opportunity for observing the Earth, Journal of Geodynamics, 49, 171–180, 2010.

Demeritt, D., Nobert, S., Cloke, H. L., and Pappenberger, F.: The European Flood Alert System and the communication, perception, and use of ensemble predictions for operational flood risk management, Hydrological Processes, 27, 147–157, 2013.

Di Baldassarre, G., Schumann, G., and Bates, P.: Near real time satellite imagery to support and verify timely flood modelling, Hydrological Processes: An International Journal, 23, 799–803, 2009.

Di Salvo, C., Ciotoli, G., Pennica, F., and Cavinato, G. P.: Pluvial flood hazard in the city of Rome (Italy), Journal of Maps, 13, 545–553, 2017.

Dottori, F. and Todini, E.: Developments of a flood inundation model based on the cellular automata approach: testing different methods to improve model performance, Physics and Chemistry of the Earth, Parts A/B/C, 36, 266–280, 2011.

Dottori, F., Alfieri, L., Salamon, P., Bianchi, A., Feyen, L., and Lorini, V.: Flood hazard map for Europe, 100-year return period, European Commission, Joint Research Centre (JRC)[Dataset] PID: http://data. europa. eu/89h/jrc-floods-floodmapeu_rp100y-tif, 2016a.

Dottori, F., Alfieri, L., Salamon, P., Bianchi, A., Feyen, L., and Lorini, V.: Flood hazard map for Europe, 50-year return period, European Commission, Joint Research Centre (JRC)[Dataset] PID: http://data. europa. eu/89h/jrc-floods-floodmapeu_rp50y-tif, 2016b.

Dottori, F., Alfieri, L., Salamon, P., Bianchi, A., Feyen, L., and Lorini, V.: Flood hazard map for Europe, 500-year return period, European Commission, Joint Research Centre (JRC)[Dataset] PID: http://data. europa. eu/89h/jrc-floods-floodmapeu_rp500y-tif, 2016c.

Dottori, F., Salamon, P., Bianchi, A., Alfieri, L., Hirpa, F., and Feyen, L.: Development and evaluation of a framework for global flood hazard mapping, Advances in water resources, 94, 87–102, 2016d.

European Commission: Directive 2007/60/EC of the European Parliament and of the Council of 23 October 2007 on the assessment and management of flood risks, J. Eur. Union, L 288, 27–34, 2007.

EWA: European Water Archive (EWA) of EURO-FRIEND-Water., URL: https: //www.bafg.de/GRDC/EN/04$_{s}pcldtbss/42_{E}WA/ewa_{n}ode.html$, 2014.

Fantini, A.: Climate change impact on flood hazard over Italy, Ph.D. thesis, University of Trieste, 2019.

Fantini, A., Di Sante, F., Coppola, E., Verdecchia, M., and Giuliani, G.: GRIPHO : a gridded high-resolution hourly precipitation dataset over Italy, in preparation, 2020.

Farr, T., Rosen, P., Caro, E., Crippen, R., Duren, R., Hensley, S., Kobrick, M., Paller, M., Rodriguez, E., Roth, L., et al.: The shuttle radar topography mission, Reviews of geophysics, 45, 2007.

Fread, D.: Channel routing, Hydrological forecasting, pp. 437–503, 1985.

Galland, J.-C., Goutal, N., and Hervouet, J.-M.: TELEMAC: A new numerical model for solving shallow water equations, Advances in Water Resources, 14, 138–148, 1991.

Gleason, C. and Smith, L.: Toward global mapping of river discharge using satellite images and at-many-stations hydraulic geometry, Proceedings of the National Academy of Sciences, 111, 4788–4791, 2014.

Grell, G., Dudhia, J., and Stauffer, D.: A description of the fifth-generation Penn State/NCAR Mesoscale Model (MM5), Tech. Rep. December, doi:10.5065/D60Z716B, 1994.

Harman, C., Stewardson, M., and DeRose, R.: Variability and uncertainty in reach bankfull hydraulic geometry, Journal of hydrology, 351, 13–25, 2008.

Havnø, K., Madsen, M., and Dørge, J.: MIKE 11–a generalized river modelling package, Computer models of watershed hydrology, pp. 733–782, 1995.

Hirt, C., Filmer, M., and Featherstone, W.: Comparison and validation of the recent freely available ASTER-GDEM ver1, SRTM ver4. 1 and GEODATA DEM-9S ver3 digital elevation models over Australia, Australian Journal of Earth Sciences, 57, 337–347, 2010.

Horritt, M. and Bates, P.: Evaluation of 1D and 2D numerical models for predicting river flood inundation, Journal of hydrology, 268, 87–99, 2002.

ISPRA, P. M. E.: Italian National Institute for Environmental Protection and Research, 2017.

Istituto di Ricerca per la Protezione Idrologica and Consiglio Nazionale delle Ricerche: Polaris - Rapporto Periodico 2017 sul Rischio posto alla Popolazione italiana da Frane e Inondazioni, Tech. rep. IRPI/CNR. URL: http://polaris.irpi.cnr.it/wpcontent/ uploads/report-2017.pdf, 2018.

Jenson, S. K. and Domingue, J. O.: Extracting topographic structure from digital elevation data for geographic information system analysis, Photogrammetric engineering and remote sensing, 54, 1593–1600, 1988.

Jing, C., Shortridge, A., Lin, S., and Wu, J.: Comparison and validation of SRTM and ASTER GDEM for a subtropical landscape in Southeastern China, International Journal of Digital Earth, 7, 969–992, 2014.

Khan, S., Hong, Y., Wang, J., Yilmaz, K., Gourley, J., Adler, R., Brakenridge, G., Policelli, F., Habib, S., and Irwin, D.: Satellite remote sensing and hydrologic modeling for flood inundation mapping in Lake Victoria basin: Implications for hydrologic prediction in ungauged basins, IEEE Transactions on Geoscience and Remote Sensing, 49, 85–95, 2011.

Krupka, M., Pender, G., Wallis, S., Sayers, P., and Mulet-Marti, J.: A rapid flood inundation model, in: Proceedings of the Congress-International Association for Hydraulic Research, vol. 32, p. 28, 2007.

Lehner, B., Verdin, K., and Jarvis, A.: HydroSHEDS technical documentation, version 1.0, World Wildlife Fund US, Washington, DC, pp. 1–27, 2006.

Lehner, B., Verdin, K., and Jarvis, A.: New global hydrography derived from spaceborne elevation data, Eos, Transactions American Geophysical Union, 89, 93–94, 2008.

Lehner, B., Verdin, K., and Jarvis, A.: HydroSHEDS Technical Documentation Version 1.2, EOS Transactions, 2013.

Leopold, L.: A View of the River, Harvard University Press, 1994.

Lighthill, M. and Whitham, G.: On Kinematic Waves. I. Flood Movement in Long Rivers, Proceedings of the Royal Society A: Mathematical, Physical and Engineering Sciences, doi: 10.1098/rspa.1955.0088, 1955.

Maione, U., Mignosa, P., and Tomirotti, M.: Regional estimation model of synthetic design hydrographs, International Journal of River Basin Management, 12, 151–163, 2003.

Marchesini, I., Rossi, M., Salvati, P., Donnini, M., Sterlacchini, S., and Guzzetti, F.: Delineating flood prone areas using a statistical approach, PeerJ Preprints, 4, e1937v1, 2016.

Marchi, L., Borga, M., Preciso, E., and Gaume, E.: Characterisation of selected extreme flash floods in Europe and implications for flood risk management, Journal of Hydrology, 394, 118–133, 2010.

Martz, L. W. and Garbrecht, J.: Numerical definition of drainage network and subcatchment areas from digital elevation models, Computers & Geosciences, 18, 747–761, 1992.

Masoero, A., Claps, P., Asselman, N. E., Mosselman, E., and Di Baldassarre, G.: Reconstruction and analysis of the Po River inundation of 1951, Hydrological Processes, 27, 1341–1348, 2013.

Merz, R. and Blöschl, G.: Flood frequency regionalisation?spatial proximity vs. catchment attributes, Journal of Hydrology, 302, 283–306, 2005.

Moel, H. d., Alphen, J. v., Aerts, J., et al.: Flood maps in Europe-methods, availability and use, Nat. Hazards Earth Syst. Sci., 9, 2009.

Montanari, A.: Hydrology of the Po River: looking for changing patterns in river discharge, Hydrology and Earth System Sciences, 16, 3739–3747, 2012.

Morelli, S., Battistini, A., and Catani, F.: Rapid assessment of flood susceptibility in urbanized rivers using digital terrain data: Application to the Arno river case study (Firenze, northern Italy), Applied Geography, 54, 35–53, 2014.

Neal, J., Schumann, G., and Bates, P.: A subgrid channel model for simulating river hydraulics and floodplain inundation over large and data sparse areas, Water Resources Research, 48, 2012.

NERC, N. E. R. C. G. B.: Flood Studies Report in Five Volumes, NERC, 1975.

Norbiato, D., Borga, M., Sangati, M., and Zanon, F.: Regional frequency analysis of extreme precipitation in the eastern Italian Alps and the August 29, 2003 flash flood, Journal of hydrology, 345, 149–166, 2007.

Pappenberger, F., Dutra, E., Wetterhall, F., and Cloke, H.: Deriving global flood hazard maps of fluvial floods through a physical model cascade, Hydrology and Earth System Sciences, 16, 4143–4156, 2012.

Paprotny, D., Morales-Nápoles, O., and Jonkman, S. N.: Efficient pan-European river flood hazard modelling through a combination of statistical and physical models, Natural Hazards and Earth System Sciences, 17, 1267, 2017.

Parsons, J. A. and Fonstad, M. A.: A cellular automata model of surface water flow, Hydrological Processes: An International Journal, 21, 2189–2195, 2007.

Rabus, B., Eineder, M., Roth, A., and Bamler, R.: The shuttle radar topography mission—a new class of digital elevation models acquired by spaceborne radar, ISPRS journal of photogrammetry and remote sensing, 57, 241–262, 2003.

Rojas, R., Feyen, L., Dosio, A., and Bavera, D.: Improving pan-European hydrological simulation of extreme events through statistical bias correction of RCM-driven climate simulations., Hydrology & Earth System Sciences, 15, 2011.

Rojas, R., Feyen, L., and Watkiss, P.: Climate change and river floods in the European Union: Socio-economic consequences and the costs and benefits of adaptation, Global Environmental Change, 23, 1737–1751, 2013.

Rudari, R., Silvestro, F., Campo, L., Rebora, N., Boni, G., and Herold, C.: Improvement of the Global Food Model for the GAR 2015, United Nations Office for Disaster Risk Reduction (UNISDR), Centro Internazionale in Monitoraggio Ambientale (CIMA), UNEP GRID-Arendal (GRID-Arendal): Geneva, Switzerland, p. 69, 2015.

Salvati, P., Bianchi, C., Rossi, M., and Guzzetti, F.: Societal landslide and flood risk in Italy., Natural Hazards & Earth System Sciences, 10, 2010.

Sampson, C., Smith, A., Bates, P., Neal, J., Alfieri, L., and Freer, J.: A high-resolution global flood hazard model, Water resources research, 51, 7358–7381, 2015.

Samuels, P.: Cross section location in one-dimensional models, in: International Conference on River Flood Hydraulics, Wiley, Chichester, pp. 339–350, 1990.

Santo, A., Di Crescenzo, G., Del Prete, S., and Di Iorio, L.: The Ischia island flash flood of November 2009 (Italy): Phenomenon analysis and flood hazard, Physics and Chemistry of the Earth, Parts A/B/C, 49, 3–17, 2012.

Sole, A., Giosa, L., Nolè, L., Medina, V., and Bateman, A.: Flood risk modelling with LiDAR technology, Flood recovery, innovation and response, 118, 27–36, 2008.

Te Linde, A., Aerts, J., and van den Hurk, B.: Effects of flood control measures and climate change in the Rhine basin, in: Proceedings of the 4th International Symposium on Flood Defence, Toronto, Canada, pp. 6–5, 2008.

Te Linde, A., Bubeck, P., Dekkers, J., De Moel, H., and Aerts, J.: Future flood risk estimates along the river Rhine, Natural Hazards and Earth System Sciences, 11, 459, 2011.

Thornthwaite, C. W., Mather, J. R., Thornthwaite, C., and Mather, J.: Instructions and tables for computing potential evapotranspiration and water balance, 1957.

Todini, E.: The ARNO rainfall—runoff model, Journal of hydrology, 175, 339–382, 1996.

Tomassetti, B., Coppola, E., Verdecchia, M., and Visconti, G.: Coupling a distributed grid based hydrological model and MM5 meteorological model for flooding alert mapping, Advances in Geosciences, doi:10.5194/adgeo-2-59-2005, 2005a.

Tomassetti, B., Coppola, E., Verdecchia, M., and Visconti, G.: Coupling a distributed grid based hydrological model and MM5 meteorological model for flooding alert mapping, Advances in Geosciences, 2, 59–63, 2005b.

Tribe, A.: Automated recognition of valley lines and drainage networks from grid digital elevation models: a review and a new method, Journal of Hydrology, 139, 263–293, 1992.

Verdecchia, M., Coppola, E., Faccani, C., Ferretti, R., Memmo, A., Montopoli, M., Rivolta, G., Paolucci, T., Picciotti, E., Santacasa, A., Tomassetti, B., Visconti, G., and Marzano, F.: Flood forecast in complex orography coupling distributed hydro-meteorological models and in-situ and remote sensing data, Meteorology and Atmospheric Physics, doi:10.1007/s00703-007-0278-z, 2008.

Verdecchia, M., Coppola, E., Tomassetti, B., and Visconti, G.: Cetemps Hydrological Model (CHyM), a Distributed Grid-Based Model Assimilating Different Rainfall Data Sources, in: Hydrological Modelling and the Water Cycle, pp. 165–201, Springer, 2009.

Wing, O. E., Bates, P. D., Sampson, C. C., Smith, A. M., Johnson, K. A., and Erickson, T. A.: Validation of a 30 m resolution flood hazard model of the conterminous U nited S tates, Water Resources Research, 53, 7968–7986, 2017.

Winsemius, H., Aerts, J., van Beek, L., Bierkens, M., Bouwman, A., Jongman, B., Kwadijk, J., Ligtvoet, W., Lucas, P., Van Vuuren, D., et al.: Global drivers of future river flood risk, Nature Climate Change, 6, 381, 2016.

Wolfram, S.: Cellular automata as models of complexity, Nature, 311, 419–424, 1984.

Wood, E., Roundy, J., Troy, T., Van Beek, L., Bierkens, M., Blyth, E., de Roo, A., Döll, P., Ek, M., Famiglietti, J., et al.: Hyperresolution global land surface modeling: Meeting a grand challenge for monitoring Earth's terrestrial water, Water Resources Research, 47, 2011.

Yamazaki, D., O'Loughlin, F., Trigg, M. A., Miller, Z. F., Pavelsky, T. M., and Bates, P. D.: Development of the global width database for large rivers, Water Resources Research, 50, 3467–3480, 2014.

Yamazaki, D., Ikeshima, D., Sosa, J., Bates, P. D., Allen, G. H., and Pavelsky, T. M.: MERIT

Hydro: a high-resolution global hydrography map based on latest topography dataset, Water Resources Research, 55, 5053–5073, 2019.

Zhao, D., Shen, H., Tabios III, G., Lai, J., and Tan, W.: Finite-volume two-dimensional unsteady-flow model for river basins, Journal of Hydraulic Engineering, 120, 863–883, 1994.